Something from nothing: linking molecules with virtual light

M. S. Rider and W. L. Barnes

Department of Physics and Astronomy, Stocker Road, University of Exeter, EX4 4QL, Devon, UK

ABSTRACT

A new research field is emerging in which ensembles of molecules are collectively hybridised with light in a process known as strong coupling. This hybridisation leads to the formation of new states that are part light and part matter, states known as polaritons. Here we offer an entry point into the field of molecular strong coupling. We include an overview of the essential phenomena and an introduction to the conceptual framework - considerable use is made of simple classical physics models since they are helpful in developing an intuitive understanding. Open questions are identified and discussed, as well as some of the exciting experimental and theoretical challenges that lie ahead.

KEYWORDS

molecule; vacuum; dipole; nanophotonics; polariton; cavity;

1. Introduction

The vacuum might not seem like a very promising material, one capable of overthrowing traditional conventions in chemistry and materials science, but that is the claim made by many who work in the embryonic field of **polariton chemistry** [1]. The key concept behind strong coupling is that a material resonance, for example an excitonic or vibrational transition in a molecule, may be hybridised with an electromagnetic mode. As a result of this hybridisation the original molecular and electromagnetic resonances are lost and two new hybrid states called polaritons are produced that are part light, and part molecule. These new states thus have very different properties from their constituents, in particular their energy levels may be very different, and the polaritons may have an extended spatial coherence. What makes molecular strong coupling remarkable is that the vacuum electromagnetic field is sufficient to produce polaritons, i.e. no 'real' light needs to be supplied. We thus have a situation where it appears that *something old + nothing = something new*; we could call it an alchemy of the vacuum[1]. This article is about trying to make sense of this seemingly paradoxical situation.

A wonderful starting point is to consider the foundational work accomplished around thirty years ago in the field of atom optics, also known as cavity quantum electrodynamics (cQED), in which excited atoms were flown under vacuum into
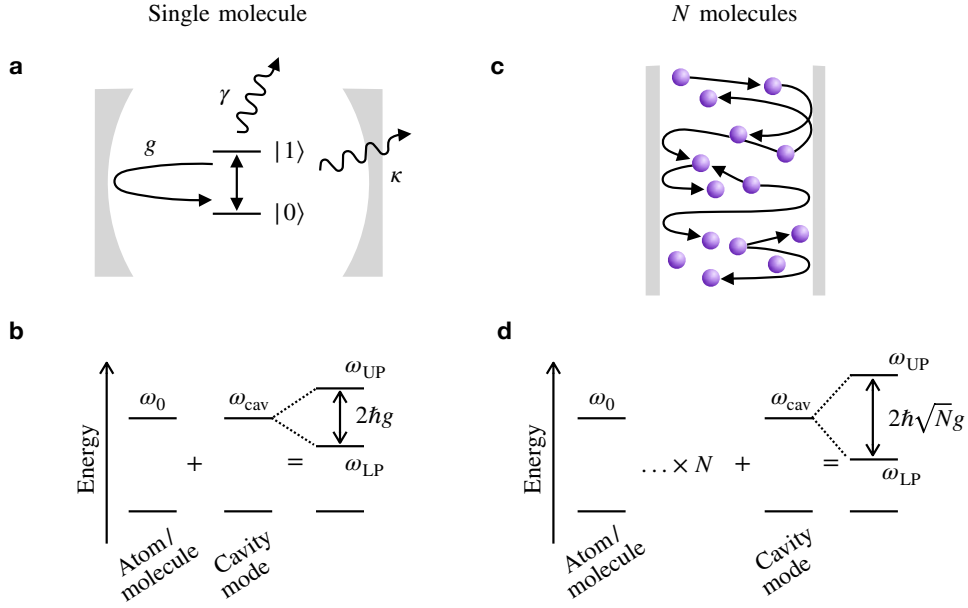
Figure 1. Linking molecules with light: Left column shows single atom/molecule cavity interaction, right column shows ensemble molecule cavity coupling. **(a)** A schematic of a single two-level system (TLS) in a cavity. The TLS and the cavity exchange a quantum of energy equivalent to the excited state energy of the TLS. The rate of exchange of this energy between the TLS and cavity is g. The decay rate of the excited state of the TLS, γ, and the decay rate of the cavity, κ, both need to be smaller than the interaction (exchange) rate g if strong coupling is to occur. **(b)** Strong coupling energy level scheme. The energy of the transition between ground and excited state of the TLS, $\hbar\omega_0$, and that of the empty cavity, $\hbar\omega_{\mathrm{cav}}$, are degenerate. When the TLS and the cavity are strongly coupled these degenerate energy levels are lost and are instead replaced by two new hybrid modes of the coupled system, the upper and lower polaritons, separated by an energy $2\hbar g$. Panels **(c)** and **(d)** show similar schematics as **(a)** and **(b)**, but this time for a situation involving a large number (N) of molecules. The separation between the upper and lower polaritons is now $2\hbar\sqrt{N}g$.

macroscopic optical cavities. A schematic of an atom optics experiment is shown in Figure 1a, where an atom is located in (more properly it travels through) the field maximum of a confocal optical cavity, e.g. formed from two highly polished mirrors.

Our analysis employs the simplest of light-matter interactions, the electric dipole interaction, i.e. the interaction between an electric dipole (matter) and an electric field (light). The electric dipole moment, $\vec{\mu}$, is that associated with the transition between the ground and excited state of the two-level system (in general this could be an atom, molecule, quantum dot etc. Here we refer to an atom - in later sections we will instead refer to 'the molecule'). This dipole moment interacts with the electric field $\vec{E}$ associated with an optical resonance, which could be that of an optical microcavity, a plasmonic nanoparticle etc.. (in what follows we will refer to this as 'the cavity mode'[2]). To keep things simple we assume that the cavity mode is a single electromagnetic mode. Both $\vec{\mu}$ and $\vec{E}$ are vector quantities, and the energy associated with their interaction is $\vec{\mu} \cdot \vec{E}$. We thus have for the coupling energy, $\hbar g$,

$$\hbar g = \vec{\mu}.\vec{E}. \tag{1}$$

We choose to write the coupling energy as $\hbar g$ because, in addition to highlighting the quantum nature of the interaction (we are dealing with atoms etc.) it is helpful to consider the rate associated with this light matter interaction, which we have written as g. Note that g is also known as the coupling strength.

When strong coupling conditions prevail, the excitation energy held by the atom can be lost to the cavity and then re-absorbed back into the atom. This cyclic exchange of energy is a hallmark of strong coupling, and occurs when the atom-cavity interaction rate for coupling between the single atom and the cavity mode, g, is such that atom and cavity have time to exchange energy coherently before, as Kimble phrased it, the "grim reaper of dissipation" takes over [2]. The cyclic exchange of energy between atom and cavity mode, known as **Rabi oscillations** [3] leads to new energy levels that are different from those of the constituent elements, see Figure 1b. The higher energy hybridised state is called the upper polariton, the lower energy one the lower polariton. The hybridised energy levels are each different from the unperturbed level by $\hbar g$ so that the total difference in energy is,

$$\Delta E = \hbar \Omega = 2 \hbar g, \tag{2}$$

where Ω is known as the Rabi frequency. The new hybrid states are of **mixed character**. Thus the photonic aspect now gains some of the attributes of matter, e.g. an effective mass, useful for example in Bose-Einstein condensation [4], whilst the matter aspect now gains some of the attributes of light, e.g. delocalised character, with great potential for intermolecular energy transfer [5]. Although we have considered here the fate of the energy held by the atom, the hybrid state is what in classical physics we refer to as a normal mode, i.e. one of the allowed modes of the system; its 'existence' does *not* require excitation energy to be pumped into the system.

What conditions does g need to satisfy if we are to ensure the interaction is in the

---

[2]Note that in the literature what we refer to here as 'the cavity mode' is also often referred to generically as 'the confined light field'.

strong coupling regime? There are two processes that compete with (i.e. may spoil) the exchange of energy between the atom/molecule and the cavity field. The first is the decay rate of the excited state of the atom, γ. If this decay rate is too fast then the molecule will lose its energy before there is time for it to be exchanged with the cavity field; we need $\gamma < g$. The second decay rate is that of the cavity mode, κ. Again, for strong coupling we need $\kappa < g$. A simple schematic indicating the different rates, g, γ, κ is shown in Figure 1a. We can thus write a simple criterion for strong coupling as,

$$\gamma, \kappa < g. \tag{3}$$

If this criterion is not satisfied, then the system is in the weak coupling regime, a regime discussed in Supplementary Information I. We note that we have assumed here that the cavity does not significantly alter the radiative decay rate, γ. This is certainly true for the large confocal cavities used in the pioneering cQED experiments depicted in Figure 1a, and discussed further in Section 6.

As we will see, when multiple atoms are involved (as in Figure 1c) the coupling strength scales with the number of atoms such that the energy level splitting becomes $2\sqrt{N}\hbar g$ (Figure 1d). This scaling with $\sqrt{N}$ is central to the polaritonic enterprise and is something we will discuss later.

At the time of writing the field is at a particularly interesting stage, with many exciting demonstrations reported, and much theoretical activity, but with many questions still wide open, and elements of controversy still to be resolved [6,7]. A clear appreciation of the underlying fundamentals is an invaluable guide in navigating this topical area, and we hope the present contribution will help in that cause.

2. Ensemble *vs.* single molecule

2.1. Conceptual perspective

$$\Omega_N = 2g_N = 2\sqrt{N}g, \tag{4}$$

where g_N is the coupling strength for N molecules. This scaling with N - compare Equation 4 with Equation 2 - is incredibly important; without it we would have no ensemble molecular strong coupling. The origin of the $\sqrt{N}$ comes from cQED theory [8], but we can use a classical argument to appreciate the result. The energy stored by a simple harmonic oscillator is proportional to the square of the oscillation amplitude, the energy stored by an oscillating electric dipole is thus proportional to its dipole moment, i.e. $\propto |\vec{\mu}|^2$, so that the energy stored by N dipole sources oscillating in phase will be proportional to $N|\vec{\mu}|^2$. We can rewrite this in terms of an effective dipole moment, $\vec{\mu}_{\text{eff}}$, with the effective dipole moment being given by $\vec{\mu}_{\text{eff}} = \sqrt{N}\vec{\mu}$. It is important to recognise that the coherent behaviour of the molecules so as to yield a giant effective dipole moment is not the only way the molecules can be linked, although it is the most evident one in most strong coupling experiments. Another type of coherent behaviour is possible, the resulting states are usually referred to as collective **dark states**. These dark states, together with other related types of non-interacting molecules, specifically

4
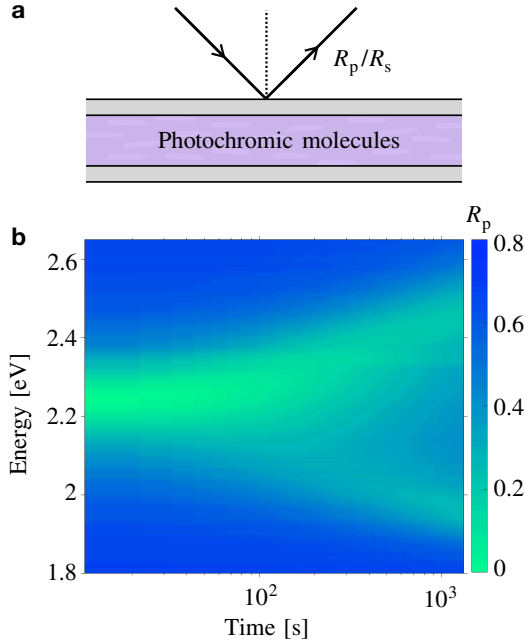
Figure 2. Transition from weak to strong coupling: (a) shows a schematic of the system, a metallic Fabry-Pérot cavity filled with photochromic spiropyran (SPI) molecules. The reflectivity at a fixed angle of incidence is measured in the experiment. **(b)** shows an example of the reflectivity data obtained, here the p-polarised reflectance is shown as a function of both photon energy and the time the sample is exposed to UV light. As the photochromic SPI molecules are exposed to UV light they undergo photoisomerisation into merocyanine (MC) molecules. MC molecules have a strong absorption in the visible so that as the number of MC molecules grows the strength of the merocyanin absorption increases, and the initial cavity mode seen as a reflection minimum around 2.2 eV evolves into two new hybrid modes. For more details see [9].

uncoupled molecules, will be discussed in Section 4.

2.2. Ensemble strong coupling as seen in experiment

At this point it is instructive to look at some experimental data on molecular ensemble strong coupling. Figure 2a shows a schematic in which a planar Fabry-Pérot type cavity with metallic mirrors is filled with a polymer matrix (PMMA) in which are dispersed spiropyran (SPI) molecules. The experiment takes advantage of the fact that when the transparent SPI molecules are exposed to UV light they undergo a photo-chemical change to merocyanine (MC), a strongly absorbing dye molecule whose absorption is centred around ~ 2.2 eV. The experiment involves measuring the reflectance (amplitude and phase) of light incident on this molecule-filled cavity. Here we show the reflectivity, R_P, at a fixed angle of incidence (65°) as a function of the time for which the sample is exposed to UV light, see Figure 2b. Initially the cavity is filled with SPI molecules, which are transparent in the visible part of the spectrum. A minimum in reflectivity is seen at around 2.25 eV, corresponding to the position of the lowest order cavity mode at this angle of incidence, achieved by selecting an appropriate cavity thickness, chosen so as to match the mode with the absorption of the MC. The sample is then illuminated with UV light, and as the SPI molecules are converted to MC molecules, the material filling the cavity goes from being transparent to absorbing. The concentration of MC molecules thus increases
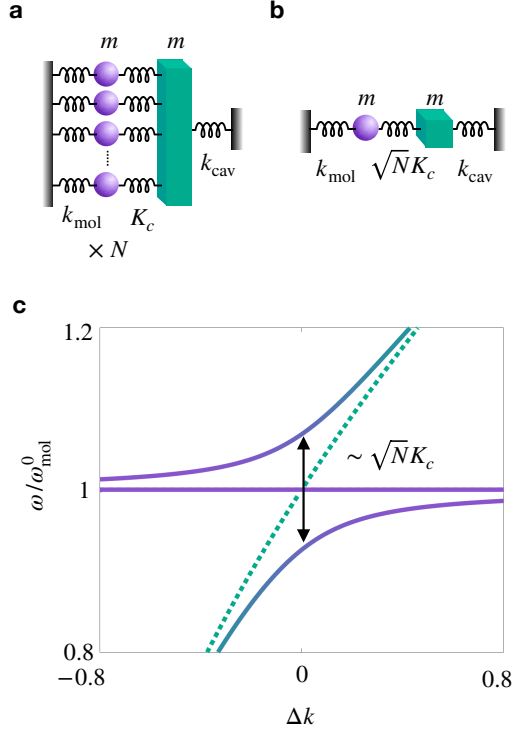
Figure 3. Coupled mechanical oscillators: (a) System of N classical oscillators with mass m and spring constant k_{mol} coupled to a single oscillator of mass m, and spring constant k_{cav} via springs with spring constants K_c. **(b)** A system of two classical oscillators both of mass m and having spring constants k_{mol} and k_{cav} respectively, coupled with a spring of spring constant $\sqrt{N}K_c$. **(c)** Dispersion relation for the system given in **(a)**. Band splitting between the two mixed modes is $\propto \sqrt{N}$, and there are $N-1$ degenerate, dispersion-less modes. The bright modes of this system correspond to the two dispersive modes of system in **(b)**.

with time, and from the data we can see that at an exposure time of ~ 200 s there are enough MC molecules in the cavity for strong coupling to occur - the cavity mode at ~ 2.2 eV splits, and two new minima in the reflectivity appear. Beyond ~ 1000 s of UV exposure (not shown) the SPI to MC conversion begins to saturate, the energy splitting at this point is ~ 0.6 eV, i.e. 25% of the unperturbed resonance energy, well into what is known as the ultra-strong coupling regime (see Section 5).

Having acquainted ourselves with some of the key strong coupling phenomena it is useful to next look at a simple model.

3. The coupled oscillator model

The value of examining a mechanical model for strong coupling is significant, and in this section we will use it to highlight some of the features of interest to us for ensemble strong coupling. Many authors have gone into great depth concerning the use of coupled mechanical oscillator models [10–12], and one can do the same thing from the perspective of coupled electronic resonances, the underlying physics is the same.

We begin by discussing a system of $N + 1$ oscillators, so as to later compare to an

6

ensemble of N molecules coupled to a single cavity mode. Note, where we talk about $N + X$ oscillators the N refers to the number of molecular oscillators and the X refers to the number of cavity mode oscillators. The two-oscillator system is most commonly used to illustrate strong coupling as this is the simplest possible system, for completeness we include a discussion of this case (i.e. $N = 1$) in Supplementary Information II.

Our mechanical oscillators are simple masses on springs. The oscillators all have the same mass m, but we distinguish between 'cavity-type' and 'molecule-type' oscillators - the cavity-type oscillators have spring constant k_{cav}, and the N molecule-type oscillators have spring constant k_{mol}. The N molecule-type oscillators are coupled to the cavity-type oscillator via springs with stiffness K_c, as illustrated in Figure 3a. In the absence of coupling ($K_c = 0$), the equation of motion (given by Newton's second law) for the cavity-type oscillator is $m\ddot{x}_{\text{cav}}(t) = -k_{\text{cav}}x_{\text{cav}}(t)$, and for the N molecule-type oscillators is $m\ddot{x}_{\text{mol}}(t) = -k_{\text{mol}}x_{\text{mol}}(t)$, such that their natural frequencies (eigenfrequencies) are $\omega_{\text{cav}}^0 = \sqrt{k_{\text{cav}}/m}$ and $\omega_{\text{mol}}^0 = \sqrt{k_{\text{mol}}/m}$ respectively. Since the oscillators are uncoupled, the frequency of oscillation of each mass is independent of the properties of the other oscillators. When coupling ($K_c \neq 0$) is introduced, the equations of motion are then,

$$m\ddot{x}_{\text{mol,i}}(t) = -k_{\text{mol}}x_{\text{mol,i}}(t) - K_c\left(x_{\text{mol,i}}(t) - x_{\text{cav}}(t)\right) \quad i \in [1, ..., N],$$
$$m\ddot{x}_{\text{cav}}(t) = -k_{\text{cav}}x_{\text{cav}}(t) + \sum_{i=1,N} K_c\left(x_{\text{mol,i}}(t) - x_{\text{cav}}(t)\right). \tag{5}$$

For solutions of the form $x_i(t) = x_i^0 e^{-i\omega t}$ (i.e. assuming the total system oscillates with a single frequency), the coupled linear equations for $x_{\text{mol,i}}^0$ and x_{cav}^0 can be written in matrix form,

$$\mathbf{M}\begin{pmatrix} x_{\text{mol,1}}^0 \\ \vdots \\ x_{\text{mol,N}}^0 \\ x_{\text{cav}}^0 \end{pmatrix} = 0, \tag{6}$$

where

$$\mathbf{M} = \begin{pmatrix} \frac{-k_{\text{mol}}-K_c}{m} + \omega^2 & 0 & ... & 0 & \frac{K_c}{m} \\ \vdots & \vdots & \ddots & \vdots & \vdots \\ 0 & 0 & ... & \frac{-k_{\text{mol}}-K_c}{m} + \omega^2 & \frac{K_c}{m} \\ \frac{K_c}{m} & \frac{K_c}{m} & ... & \frac{K_c}{m} & \frac{-k_{\text{cav}}-K_c}{m} + \omega^2 \end{pmatrix}. \tag{7}$$

Non-trivial solutions exist for $\det(\mathbf{M}) = 0$, which leads to the condition that

$$\omega^2 = \frac{1}{2}\left[\omega_{\text{mol}}^2 + \omega_{\text{cav}}^2 \pm \sqrt{\left(\omega_{\text{mol}}^2 - \omega_{\text{cav}}^2\right)^2 + 4N\Gamma^2}\right] \text{ and } \omega_{\text{mol}}^2 \ (N-1 \text{ times}), \tag{8}$$

where

$$\omega_{\text{mol}} = \sqrt{\frac{k_{\text{mol}} + K_c}{m}}, \quad \omega_{\text{cav}} = \sqrt{\frac{k_{\text{cav}} + K_c}{m}}, \quad \Gamma = \frac{K_c}{m}. \tag{9}$$

We find three unique eigenvalues: two describing the **mixed states** (hybrid states whose eigenvalues are a superposition of both cavity- and molecule-type oscillators) and $N - 1$ degenerate **dark states** (states whose eigenvalues are a superposition of only one type of oscillator, in this case molecule-type oscillators). The eigenvalues for $N = 20$ are plotted in Figure 3c. A casual glance at the $N - 1$ degenerate eigenvalues makes these states seem no different to uncoupled states[3]. However these $N - 1$ degenerate eigenvalues, ω_{mol}, are best understood by studying their $N - 1$ unique eigenvectors, $(x_{\text{mol},1}, x_{\text{mol},2}, ..., x_{\text{mol,N}}, x_{\text{cav}})^T$, in which $x_{\text{cav}} = 0$ and $\sum_{i=1}^{N} x_{\text{mol},i} = 0$. The two mixed states demonstrate the behaviour $x_{\text{mol,i}} = x_{\text{mol}}$ for all i. If we only wish to study the mixed states, this property gives us a useful shortcut. By only studying motion in which the displacements of all of the molecule-type oscillators are the same, $x_{\text{mol,i}} = x_{\text{mol}}$, the system then reduces to two distinct equations to solve,

$$m\ddot{x}_{\text{mol}}(t) = -k_{\text{mol}}x_{\text{mol}}(t) - K_c \left(x_{\text{mol}}(t) - x_{\text{cav}}(t) \right) \tag{10}$$

$$m\ddot{x}_{\text{cav}}(t) = -k_{\text{cav}}x_{\text{cav}}(t) + NK_c \left(x_{\text{mol}}(t) - x_{\text{cav}}(t) \right), \tag{11}$$

which, writing in matrix form and solving for ω, we find,

$$\omega_{\pm}^2 = \frac{1}{2} \left[\omega_{\text{mol}}^2 + \omega_{\text{cav}}^2 \pm \sqrt{\left(\omega_{\text{mol}}^2 - \omega_{\text{cav}}^2 \right)^2 + 4N\Gamma^2} \right], \tag{12}$$

These eigenvalues are the same as those of a two-oscillator system (discussed in more detail in Supplementary Information II), provided we make the transformation $K_c \rightarrow \sqrt{N}K_c$. Thus, if we are only interested in the mixed/hybrid states of the $N+1$ oscillator system we can use the effective two-oscillator model shown in Figure 3b.

We note that ω_{mol} and ω_{cav} are the frequencies of each oscillator if the position of the other oscillator were to remain fixed. For $k_i \gg K_c$, $\omega_i \approx \omega_i^0$, and the natural frequencies of the uncoupled oscillators are retained. We see in Figure 3c that the introduction of the third spring results in an avoided crossing at resonance. The splitting at resonance is given by $\omega_+^2 - \omega_-^2 = 2K_c/m$. At resonance, such that $\omega_{\text{mol}} = \omega_{\text{cav}}$, in the uncoupled system we would see the two masses oscillating with the same frequency but with arbitrary relative phase. In the coupled system, the two normal modes are given by: the masses oscillating in phase (lower energy) or out of phase (higher energy).

Our treatment here has assumed that the N oscillators are indistinguishable; in practice this is unlikely to be the case, but extensions to the approach outlined here can be can be made, for example to include a distribution of oscillator resonance frequencies (inhomogeneous broadening). The simplicity of the model employed so far makes this comparison between classical and quantum pictures relatively straightforward, and is our next topic.

---

[3]See Section 4 for a discussion on the difference between these types of state.

3.1. Quantum vs classical oscillators

The quantum 'equivalent' of Newton's second law is the Schrödinger equation, where, instead of thinking of the equations of motion, we think about the evolution of the quantum state, $|\Psi\rangle$, such that $\mathbf{H}|\Psi\rangle = i\hbar\partial_t|\Psi\rangle$. The total system state of N molecules and one cavity mode can be written as $|\Psi\rangle = \sum_{i=1,N} a_{\mathrm{mol},i}(t)|\Psi_{\mathrm{mol},i}\rangle + a_{\mathrm{cav}}(t)|\Psi_{\mathrm{cav}}\rangle$, where $a_{\mathrm{mol,i}}(t)$ and $a_{\mathrm{cav}}(t)$ are complex time-dependent coefficients. We can write the coefficients in vector form, $\mathbf{A} = [a_{\mathrm{mol},1}(t), a_{\mathrm{mol},2}(t), ..., a_{\mathrm{mol,N}}(t), a_{\mathrm{cav}}(t)]^T$. Making an analogy to the classical system, we can write $\mathbf{MA} = 0$, where $\mathbf{M}$ is the quantum coupling matrix,

$$\mathbf{M} = \begin{pmatrix} \omega_{\mathrm{mol}} - \omega & 0 & ... & 0 & g \\ \vdots & \vdots & \ddots & \vdots & \vdots \\ 0 & 0 & ... & \omega_{\mathrm{mol}} - \omega & g \\ g & g & ... & g & \omega_{\mathrm{cav}} - \omega \end{pmatrix}. \tag{13}$$

which when solved for the system eigenvalues, ω, gives

$$\omega_{\pm} = \frac{1}{2}\left[\omega_{\mathrm{mol}} + \omega_{\mathrm{cav}} \pm \sqrt{(\omega_{\mathrm{mol}} - \omega_{\mathrm{cav}})^2 + 4Ng^2}\right], \quad \omega_{\mathrm{mol}} \ (N-1 \text{ times}), \tag{14}$$

with splitting between the two mixed modes at resonance given by the Rabi frequency $\Omega_N = 2\sqrt{N}g = 2g_N$, in agreement with Section 2. The $N-1$ dark modes have frequency ω_{mol}. The molecular mode is defined by the transition dipole moment between the ground and excited state of a particular molecular resonance. The transition dipole moment is given by $\vec{\mu}(t) = e\langle g|\vec{r}|e\rangle \exp(i\hbar\omega_{\mathrm{mol}}t)$, where $\vec{r}$ is the displacement vector and $\hbar\omega_{\mathrm{mol}}$ is the energy of the transition involved, and e is the electronic charge.

The physical interpretation of the molecular dark states can be understood by comparison to the mechanical oscillator example, but instead of the displacement of the oscillators, the net vector of the individual dipole moments in relation to the polarisation vector of the light can be considered. We can see how the classical and quantum coupling matrices are mapped onto to each other by comparing Equation (7) (classical) with Equation (13) (quantum). We can thus transform the classical into a quantum coupling matrix, this is done in Supplementary Information III.

4. Bright, dark, and uncoupled states

In most experiments on strong coupling, **uncoupled** and **dark** states look very similar, a dispersion-less resonance centred around the original molecular resonance frequency ω_{mol}; here we revisit the system of $N+1$ coupled mechanical oscillators to examine the differences between uncoupled and dark states.
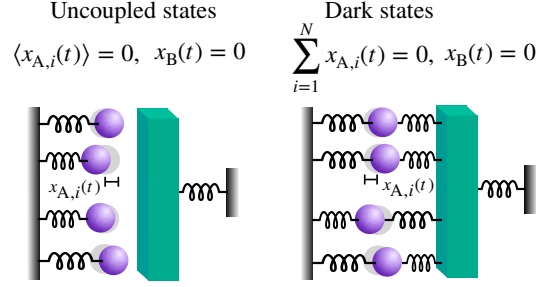
4.1. Uncoupled states

Uncoupled molecular states are perhaps the easiest to interpret; we remove the coupling springs, or mathematically take springs with $K_c = 0$. Exciting a molecule-type oscillator will not affect the cavity-type oscillator, and so we can assume $x_{\mathrm{cav}}(t){=}0$, see Figure 4. When energy is supplied to the N molecule-type oscillators, they may oscillate with arbitrary phase in relation to one another. On average each oscillator has zero time-average displacement, but at any given moment their collective net displacement may be non-zero. On a dispersion diagram this will be seen as a band of N degenerate modes of frequency ω_{mol}^0.

4.2. Dark states

Dark states are often described as any non-bright (non-radiative) state. However in the context of polaritonic systems, it is important to distinguish between uncoupled states and dark collective states which – from here onwards – we refer to as dark states. Dark states are collective states of the coupled system ($K_c \neq 0$) to which the cavity-like oscillator has zero contribution. Unlike mixed states (*aka* bright states), exciting molecule-type oscillators in a dark state **does not** impart energy to the cavity-type oscillator; thus we again take $x_{\mathrm{cav}}(t) = 0$. There are $N-1$ dark states for which $\sum_{i=1}^{N} x_{\mathrm{mol},i} = 0$, with eigenvalue ω_{mol} ($\approx \omega_{\mathrm{mol}}^0$ for $K_c \ll k_{\mathrm{mol}}$ as described in Section 3, the equivalence is exact for the quantum mechanical case). The net displacement of the molecule-type oscillators must be 0 at all times, to maintain the condition $x_{\mathrm{cav}}(t) = 0$; their **collective motion** maintains this condition. This is in contrast to a bright state, in which $x_{\mathrm{cav}}(t) \neq 0$. A simple example is that of a three-oscillator system (two molecule-type oscillators coupled to one cavity-type oscillator) in which $x_{\mathrm{mol},1}(t) = -x_{\mathrm{mol},2}(t)$. One way to formulate the basis of $N-1$ dark states is through $x_{\mathrm{mol},1}(t) = -x_{\mathrm{mol},i}(t)$ for $i \neq 1$, $x_{\mathrm{mol,j}}(t) = 0$ for $i \neq j$. A basis change can give dark states which are delocalised over many oscillators. We can also use a basis change such that the greatest displacement is on a single oscillator, and the negative displacement is evenly distributed over many or all other oscillators. For large N, this tends to an entirely local basis. So, dark state excitations can be modelled as **delocalised** or **localised** states; the most appropriate basis to use depends on how the system is initially excited, e.g. if energy enters the system via a small subset of spatially-close oscillators then a local basis may be the most appropriate. In molecule-light systems, all molecules are generally excited at the same time, so the delocalised basis may be employed. However in disordered systems the dark states can become semi-localised [13]. The time-scales of the system dynamics are important, as dephasing is likely to be very quick, leading to dark states acting as uncoupled states.

The **reservoir** is a term sometimes used to refer to the system of many molecular dark states (i.e. the very large N as found in most experiments), and can refer to uncoupled states, collective dark states or a mixture of both. For the reservoir concept to work, the number of molecules should be large enough that exciting a given state does not significantly increase the macroscopic temperature of the system, in line with the thermodynamic definition of a reservoir.

Uncoupled states

$\langle x_{A,i}(t)\rangle = 0, \; x_B(t) = 0$

Dark states

$\sum_{i=1}^{N} x_{A,i}(t) = 0, \; x_B(t) = 0$

Figure 4. Uncoupled *vs.* dark states of mechanical oscillators: Mechanical oscillator model to describe uncoupled states and dark states. On the left is the situation for uncoupled states – there is no spring connecting the molecular resonators (purple) to the cavity resonator (green). On the right is the situation for dark states. Here the molecular resonators are coupled to the cavity resonator, but the net amplitude of the motion of the molecular resonators remains zero (hence dark).

4.3. Single molecules or collective mode?

In the previous sections we discussed how an effective $1 + 1$ model can be used to calculate the mixed modes of a coupled system, this reduced the computational effort required to study the full $N + 1$ system, but at the cost of ignoring the dark states. For light-molecule systems, this effective theory comes from treating the molecules via their collective dipole moment such that $g_N = \sqrt{N}g$.

It is interesting to ask whether this method is always successful in capturing the behaviour of the system, and if not, when should caution be advised. For realistic planar cavities the dark modes are not present in the dispersion relation due to absorption, and due to an impedance mismatch preventing a significant amount of light entering the cavity around the frequency of the molecular/dark mode resonance, see e.g. [14], Figure 3b. It could thus be argued that a focus on just the mixed modes gives a reasonable description of the system, at least when calculating the dispersion relation. In systems with differing confined light modes, for example surface plasmons on interfaces, then dark states may be seen in the experimentally obtained dispersion relation, see [15] Figure 1c. As uncoupled molecules and dark states have the same frequency, one 'trick' to recover the full dispersion relation is to include an additional uncoupled resonance in the system at the molecular frequency [16]. Whilst the eigenstates of this composite system are not the same as for the full $N + 1$ system, many useful observables can nonetheless be calculated.

When more complex systems such as molecules coupled to surface plasmons on gratings are considered, the $1 + X$ effective model (i.e. we consider just one molecular mode, the collective (bright) molecular 'mode', and X photonic modes) fails to correctly reproduce experimental results, even with the addition of an uncoupled molecular resonance. The full basis of photonic and molecular states must thus be considered to describe the optical properties of such systems correctly [17]. For a grating supporting forward and backward propagating SPs (i.e. where $X = 2$), the final system will be described by a basis of 4 bright states and $N - 2$ dark states. One way in which these states can be calculated is by including the full set of N molecular states in the single-particle basis, which also has the advantage of allowing one to include molecule-dependent variations into the model, e.g. inhomogeneous broadening. Whilst a full analytical solution may be overly cumbersome, numerical solutions should be tractable.

5. Choice of strong coupling criterion

In Section 1 we introduced a simple criterion for atom-light strong coupling with,

$$\text{Strong coupling condition 1}: \quad g > \gamma, \kappa, \quad \quad \quad (3 \text{ revisited})$$

where the decay rate of the excited state of the atom is γ, and κ is the decay rate of the cavity mode. (Strictly speaking κ and γ are dephasing rates, see Supplementary Information IV.) The cavity losses are due to absorption and the leaking of energy into the environment, while the atomic losses are due to spontaneous emission as the atom relaxes from its excited state to the ground state; for more complicated electronic states such as those involving molecules, energy can also be lost non-radiatively.[4] Since both γ and κ represent losses, a system with no losses will be in the strong coupling regime for an arbitrarily small value of g. When losses are included a variety of criteria for strong coupling have been discussed, we now look at these alternatives by making use of the quantum oscillator model for molecules coupled to a cavity as discussed in Section 3.1.

Losses can be added as imaginary components of frequency, which lead to a decay in the amplitude of the associated wavefunction such that $e^{-i\hbar\omega_{\text{mol}}t} \rightarrow e^{-i\hbar(\omega_{\text{mol}}-i\gamma)t} = e^{-i\hbar\omega_{\text{mol}}t-\hbar\gamma t}$, and similarly $e^{-i\hbar\omega_{\text{cav}}t} \rightarrow e^{-i\hbar\omega_{\text{cav}}t-\hbar\kappa t}$. The mixed states of the molecule-cavity system will then have modified frequencies, given by an appropriately modified version of Equation (14), i.e,

$$\omega_{\pm} = \frac{1}{2}\left[\omega_{\text{mol}} - i\gamma + \omega_{\text{cav}} - i\kappa \pm \sqrt{(\omega_{\text{mol}} - i\gamma - \omega_{\text{cav}} + i\kappa)^2 + 4g^2}\right]. \quad (15)$$

This results in modes with finite width, as found in measurements of optical properties such as reflection, transmission and phase. An effective dispersion plot can be produced by plotting the lineshape[5], see Figure 5a. We have taken the loss rates as $\hbar\kappa = 0.01$ eV and $\hbar\gamma = 0.001$ eV. At resonance, i.e. where $\omega_{\text{mol}} = \omega_{\text{cav}}$, the Rabi splitting, modified by losses, is given by,

$$\omega_{+} - \omega_{-} = \sqrt{4g^2 - (\gamma - \kappa)^2} = 2g\sqrt{1 - \frac{(\gamma - \kappa)^2}{4g^2}} = \Omega. \quad (16)$$

We see that the presence of damping reduces the Rabi splitting. The expected splitting (namely the real component of Ω) as a function of g is shown in Figure 5b (solid black line). For $\gamma = \kappa$ the contributions from the two decay rates exactly cancel, giving the lossless case $\Omega = 2g$, (dotted black line). The presence of non-equal loss mechanisms means that a non-zero value of g is required in order to have a non-zero Rabi splitting. We can consider the following candidate criteria for strong coupling as [18–20],

$$\text{Strong coupling condition 2}: \quad g^2 > (\gamma - \kappa)^2/4. \quad (17)$$

The onset of this condition is given as a solid purple line in Figure 5b. This definition

---

[4]For the mechanical oscillator model discussed in this section, losses are usually in the form of friction.

[5]The lineshape is given by $[(\omega - \omega_{+})^2 + 4(\alpha\gamma + \beta\kappa)^2]^{-1} + [(\omega - \omega_{-})^2 + 4(\alpha\gamma + \beta\kappa)^2]^{-1}$, where α and β are the molecular and photonic weights of each mode respectively, and $\alpha + \beta = 1$. At zero detuning, $\alpha = \beta = 1/2$.

does not take into account the additional need to overcome the linewidths of the new modes in order to observe the splitting, and so, as seen in the amplitude plotted in Figure 5c, no splitting is seen at the onset of this condition. We can define a new condition in which we demand that the splitting is greater than the combined linewidths of the modes, such that $\text{Re}(\Omega) > (\gamma + \kappa)$. This gives the new condition (or rather, a rule of thumb), as,

$$\textbf{Strong coupling condition 3}: \quad g^2 > \frac{\gamma^2 + \kappa^2}{2}. \tag{18}$$

This condition is shown as a solid blue vertical line in Figure 5b. The expected amplitude of the lineshape on resonance for this system is given for the values of g required for the onset of strong coupling conditions 2 and 3 in Figures 5c and d respectively. Whilst the energy level splitting is real at a relatively small value of g (i.e. condition 2), no splitting is observed. At the onset of condition 3 a very small local minimum is observed. Far above condition 3, as illustrated in Figure 5e, two distinct peaks separated by a local minimum can be observed.

The conditions above are different from the more-often expressed condition,

$$\textbf{Strong coupling condition 4}: \quad g > (\gamma + \kappa)/2, \tag{19}$$

which is similar in spirit to condition 3, except that it is first assumed that the splitting is simply $2g$, rather than $\text{Re}(\Omega)$.

In practice the distinction between these different regimes may not always be important. In a system which meets the strong coupling regime as measured against one of the conditions mentioned above, but not against those of another, then the system is perhaps only marginally in the strong coupling regime; energy may only have been exchanged between the two subsystems for a single oscillation. Often experiments easily reach the strong coupling regime so that the exact point of transition from weak to strong coupling is not particularly important. See also Supplementary Information IV.

When the coupling strength is much greater than that needed to ensure that the strong coupling regime is attained then a regime beyond strong coupling may be entered, called **ultrastrong coupling** [21,22]. Rather arbitrarily the criterion for being in this regime is that the splitting is $> 10\%$ of the transition energy. As we have seen in Section 2, this is often easily achieved. Perhaps the most intriguing aspect of this regime is that the ground state of the molecular system is predicted to be modified, the interaction with the field is sufficient to (partially) hybridise the vacuum with the ground state. A system in which the coupling strength (and thus energy level splitting) exceeds the transition energy is said to have achieved deep strong coupling [23]. While this has not yet been achieved with the electronic state of a material, success has been found using metamaterials [24].

6. Quantitative analysis of experiments

We now take a quantitative look at two representative examples of strong coupling between atoms/molecules and cavity modes; the examples are chosen for their didactic
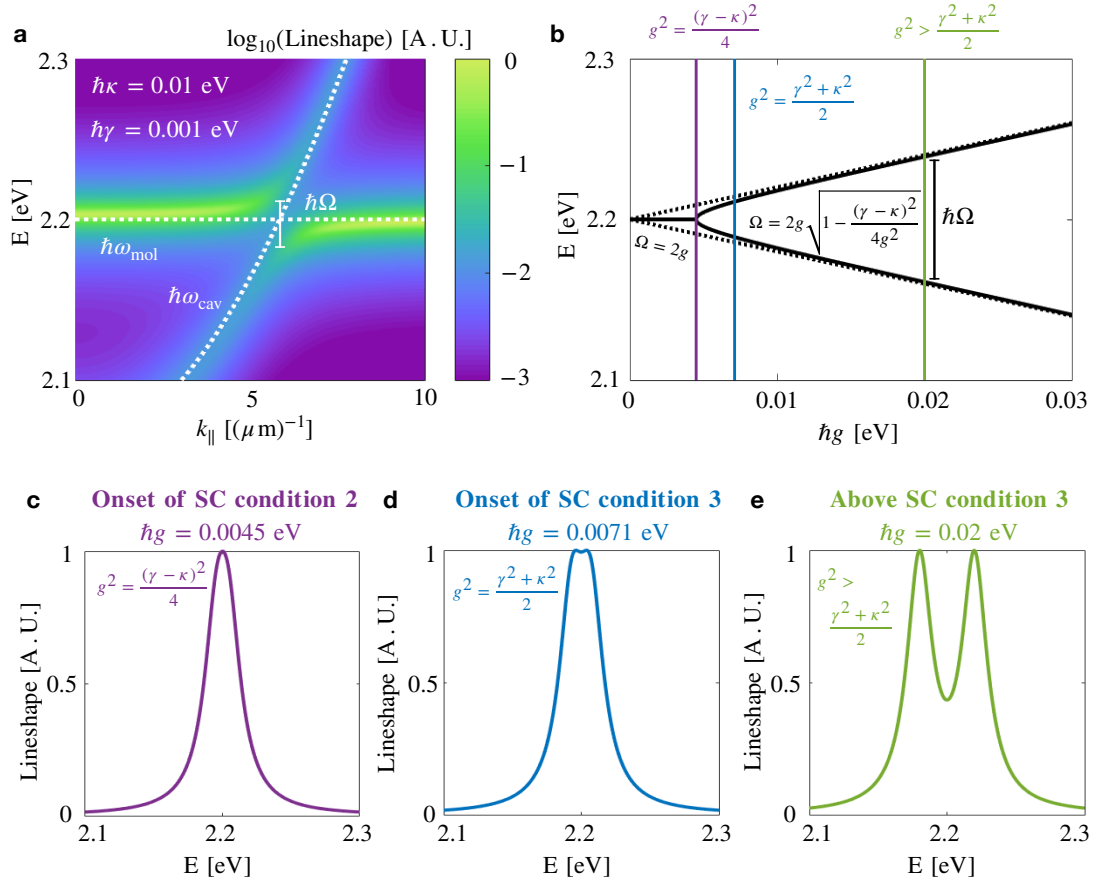
Figure 5. Including losses: (a) Dispersion relation for molecules in a cavity for $\hbar g = 0.02$ eV. **(b)** Ω as a function of g. Vertical lines denote different conditions of g. SC2 in purple, SC3 in blue, and situation in (a) given by green. **(c)-e** give the normalised lineshapes at resonance for the three conditions.

value. First we look at atom strong coupling experiments from the era of cavity-QED. Second we focus on a planar Fabry-Pérot microcavity experiment where the cavity was filled with molecules, and the strong coupling involved molecular vibrational resonances.

We want to be able to check whether the strong coupling condition 1 is satisfied, i.e. whether or not $\gamma, \kappa < g$. In a typical experiment g, γ, κ are experimentally derived quantities, albeit often indirectly. We would also like to compare the measured value of g (inferred from the Rabi splitting measured in an experiment) to the value calculated from the system parameters using Equation (22) below. To predict Ω there are four quantities that we need to keep track of in each of the experiments we analyse, these are: the mode volume (and hence vacuum field strength, E); the number of molecules involved, N; the cavity quality factor Q of the cavity resonance, and the dipole moment of the molecular transition, $\vec{\mu}$. Before we look at our chosen experiments it is useful to consider some of these parameters in more detail.

6.1. Mode volume and vacuum field strength

For our present analysis we assume that we have just one cavity mode to consider, for example the lowest order mode of a planar Fabry-Pérot microcavity as shown in Figure 2a. Fundamental to the idea of using strong coupling to modify physical, chemical and material properties is that such effects do **not** rely on us injecting light (as is the case for example in laser-controlled chemistry [25]). Instead, the electric field giving rise to strong coupling is the vacuum field. For what we wish to accomplish here it is convenient to consider this vacuum field as some kind of electromagnetic noise; the uncertainty principle prohibits space from being quiet!. Whilst the mean value of this random field is zero, its RMS value is not zero. (It is this same electromagnetic vacuum noise that helps to drive spontaneous emission.) Here it is sufficient to know that in quantum mechanics the ground state of each mode of the vacuum field can be considered to have an energy $\hbar\omega/2$, where ω is the (angular) frequency associated with the mode.

Assuming that we can consider our system (a filled cavity) to be spatially homogeneous and to be filled with empty space (both clearly not true, but..) then the energy density associated with this EM field is known from classical electromagnetism [26] to be $\varepsilon_0 E_{\mathrm{RMS}}^2$, and the energy associated with the cavity mode is thus $\varepsilon_0 E_{\mathrm{RMS}}^2 V$, where V is the cavity mode volume. Equating this to the vacuum energy of the mode, $\hbar\omega/2$, we find the vacuum field strength associated with the cavity mode to be,

$$E_{\mathrm{RMS}} = \sqrt{\frac{\hbar\omega}{2\varepsilon_0\varepsilon_{\mathrm{b}}V}}, \tag{20}$$

where now ε_{b} is the background permittivity of the cavity-filling material. Combining Equations (20) and (1) we find the single molecule coupling strength to be,

$$g = \mu\sqrt{\frac{\omega}{2\varepsilon_0\varepsilon_{\mathrm{b}}\hbar V}}. \tag{21}$$

For a given molecular transition of dipole moment μ in a cavity of mode volume V, Equation (21) allows us to calculate the corresponding coupling strength g. If we find

that $\gamma < g$ then single molecule strong coupling is possible, provided $\kappa < g$. If $\gamma, \kappa \not< g$ then it may still be possible to reach the strong coupling regime by increasing the number of molecules, i.e. making use of the $\sqrt{N}$ scaling factor discussed in Section 2. Let us now look more closely at the N molecule case.

6.2. The number of molecules N and the ensemble perspective

For an ensemble of N molecules, and bearing in mind our earlier discussion about the effective dipole moment, the coupling strength can be expressed as,

$$g_N = \sqrt{N}g = \mu \sqrt{\frac{N}{V} \frac{\omega}{2\varepsilon_0 \varepsilon_b \hbar}}. \tag{22}$$

We see that provided our molecules fill the mode volume, the coupling strength scales with the square root of the molecular concentration $\sqrt{N/V}$. This scaling is an oft-used test for the strong coupling regime, where the energy-level splitting is measured as a function of the molecular concentration [27].

6.3. Cavity decay rate and Q-factor

There is another powerful message we can extract from Equation (22); if we want to modify material properties, for example by trying to change the relative energy of singlet and triplet states in a light-emitting material as a result of hybridisation [28], then the energy shift, $\hbar g_N$, needs to be a substantial fraction of the transition energy, $\hbar\omega_0$. For example, a shift of 0.2 eV for a transition energy of 2.0 eV requires $g_N/\omega_0 \sim 0.1$. Noting that strong coupling requires $\kappa < g_N$, and that by extension $\kappa/\omega = 1/2Q < g_N/\omega$ we see that in the realm of polaritonic chemistry we need $2Q > \omega/g_N$, where Q is the quality factor of the cavity mode. Thus for a 10% change in energy level, i.e. $g_N/\omega \sim 0.1$, we need our cavity mode to have a quality factor of only $Q \geq 5$! This is in stark contrast to the cQED case of atom optics where a Q of $\sim 10^8$ was required to achieve single atom strong coupling (and was a major technical challenge). The photonic requirements for strong coupling in the ensemble case are in general not challenging, indeed, $Q \sim 10 - 100$ is a typical requirement, and can even be achieved with lossy plasmonic modes, a wide range of plasmonic materials and structures may thus be employed. An additional attraction is that plasmonic modes may be used to help achieve extreme light confinement, thus enabling single molecule strong coupling to be achieved [29].

We can look at the use of low-Q cavity modes from another perspective. Molecules are a very different proposition to atoms for strong coupling; atomic transitions are very narrow ($\sim 10^7$ Hz), whilst molecular transitions are typically very broad ($\sim 10^{13-14}$ Hz). To achieve molecular strong coupling, where linewidths are broad, we **need** to use low-Q cavity modes otherwise the full molecular response cannot be encompassed by the cavity mode. Whilst all of this seems very promising for molecular strong coupling, the use of low-Q cavity modes comes at a price. The associated high values of κ correspond to cavity decay times of order 10 fs. It remains an open question as to what the full implications of this very rapid timescale may be for the kinds of chemistry that might be modified by strong coupling.

6.4. Dipole moment

The dipole moment can not usually be determined from measurements carried out as part of a strong coupling experiment, in atom optics it may be obtained from other sources, in the ensemble case it can often be obtained from (optical) extinction measurements. Here we will make the best estimates we can, bearing in mind that our objective is to establish some order-of-magnitude comparisons between theory and experiment.

6.5. Strong coupling experiments involving atoms and cavity QED

We begin by looking at single atom strong coupling. Intense activity during the 1980s and 1990s was expended on reaching the strong coupling regime for just a single atom in a cavity [30] so as to test many of the foundational aspects of quantum mechanics, the work was rewarded with a Nobel prize in 2012. Our interest in the present article however lies in the opposite direction, that of embracing a large number of molecules. For this reason it makes sense here to begin by examining one of these early 'multi-atom' experiments reported by Kaluzny *et al.* [31], work that involved cavities containing sodium (Na) atoms. The transition involved was a Rydberg transition between the $36S_{1/2}$ and $35P_{1/2}$ states of atomic sodium, corresponding to a frequency (wavelength) of 82 GHz (24.5μ m), i.e. in the microwave regime[6]. In this particular experiment a beam of atoms was prepared in the $36S_{1/2}$ state and then injected into the cavity. When the atoms emerged from the cavity a detector was used to determine how many of them were in the excited ($36S_{1/2}$) and ground ($35P_{1/2}$) states as a function of the time that they interacted with the cavity. If the coupling (interaction) rate between the excited atoms and the cavity was greater than the rates of dissipation of both the cavity mode, κ, and decay of the upper Rydberg state of the Na atom γ, then, as we noted above, we expect that the energy should oscillate back and forth between the cavity mode and the atoms, resulting in a periodic modulation of the fraction of atoms in the excited state.

Data for the evolution of the excited state population in the experiment of Kaluzny *et al.* are reproduced in Figure 6 panel (a), for the case of 40,000 atoms in the cavity. A clear oscillation can be seen in the excited state population as a function of interaction time, suggesting that the exchange rate dominates over the dissipation rates. Moreover, we note that the results for other numbers of atoms in the cavity also exhibited an oscillatory excited state population, the oscillation period becoming longer as the number of atoms is reduced. Eventually, as the number of atoms is reduced sufficiently, the oscillations are no longer seen because the cavity damping rate dominates; this was the case in this particular experiment when there were 4000 atoms in the cavity[7]. The results from this pioneering experiment beautifully show the coherent exchange of energy between the atoms and the cavity mode, indicating that they have indeed formed a new hybrid state that is part light, part matter.

In panel (b) of Figure 6 we show data from the experiment of Thompson *et al.* [30] that involved looking at the spectral transmission of a cavity containing just one caesium (Cs) atom, employing the Cs $6S_{1/2}$ and $6P_{3/2}$ transition at a wavelength of

---

[6]Note that Rydberg states continue to be an important testing ground for strong coupling physics, see [32].

[7]Note that making a quantitative connection between the oscillations seen in panel (a) and the predicted Rabi frequency is quite subtle, see [31] for details.
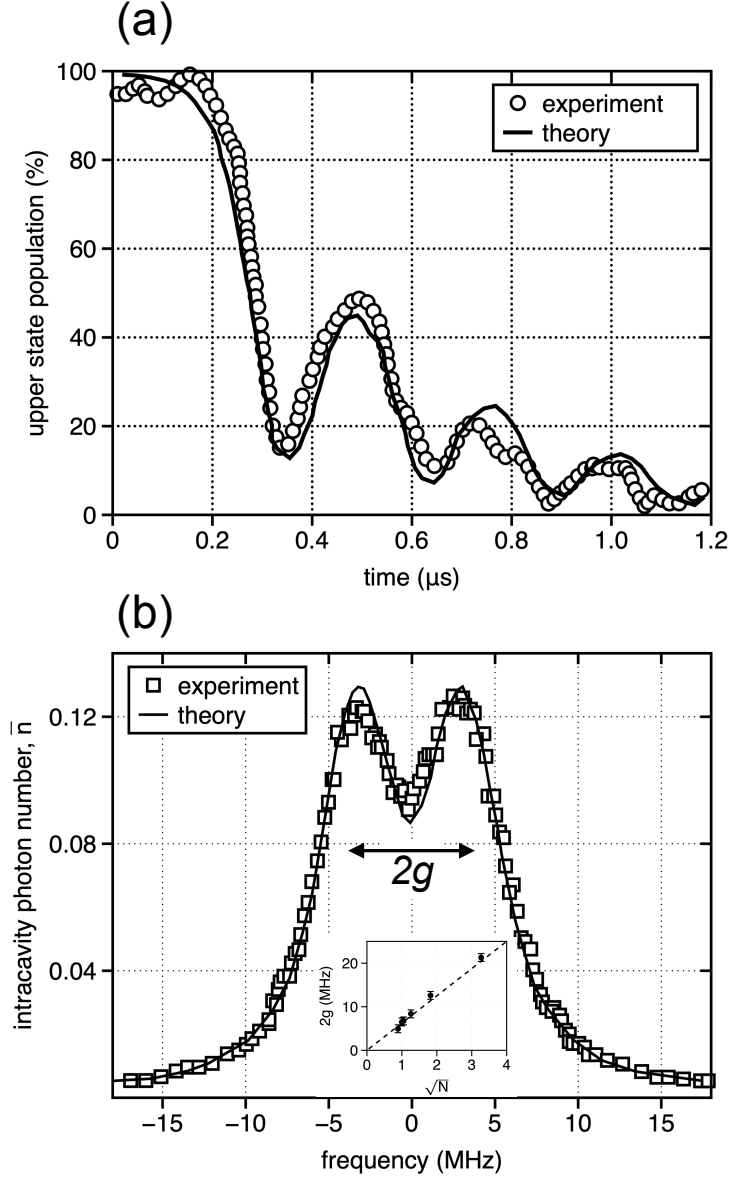
Figure 6. Atom cavity-QED: (a) Kaluzny *et al.* The measured upper Rydberg-state population of Na atoms flown through a cavity resonant with the Rydberg transition, as a function of the time the atoms interacted with the cavity, shown as circles. The associated theoretical model is shown as a line. Data are adapted from [31]. The oscillation shows the exchange of energy between the atoms and the cavity as a result of strong coupling. **(b) Thompson *et al.*** The measured average photon number $\bar{n}$ in cavity through which Cs atoms fly, shown as a function of angular frequency, more particularly in terms of the de-tuning from the empty cavity resonance frequency. The boxes give an indication of the error bars. The line is a best fit by the authors using an analytic expression for the cavity transmittance. Data are adapted from [30]. The frequency splitting of the cavity transmission peak ($2g$) arising from strong coupling is shown. The inset shows how the measured splitting varied with the square root of the number of atoms in the cavity.

852 nm. Here we see that the isolated cavity mode has been split into two as a result of coupling between the atom and the cavity mode, evidence that here too the exchange rate is greater than the dissipation rates. These authors also looked at changing the number of atoms in the cavity, and found that the splitting became greater and better defined as the number of atoms was increased, this is also shown in panel (b). This experiment thus nicely shows the change in energy levels of the hybrid atom-cavity states, complimenting the demonstration of coherence in the work of Kaluzny *et al.*, shown in panel (a). Note that the change in energy between the uncoupled atoms and the newly created hybrid states is very modest, $\delta E/E \sim 10^{-8}$, interesting for atom optics, but orders of magnitude away from allowing us to contemplate changing the energy level structure of molecules. However, as with the results on coherent energy exchange in panel (a), the resolution to this problem is already present in the data from both Kaluzny *et al.* and Thompson *et al.*, both the exchange rate and the energy level changes increase as the number of atoms increases, this is shown in the inset in panel (b).

Now let us look at the numbers that relate to the splitting seen in Figure 6b. In atom optics it is usual to work with frequency, so that the Cs transition occurs at 352 THz. Since our formulae, as is common, are in terms of angular frequency, then we can write the angular frequency as $2\pi(352)$ THz. Thompson *et al.* give the values of $g, \gamma_\perp, \kappa$ (see Supplementary Information IV re: $\gamma_\perp$) as: $g = 2\pi(3.2 \pm 0.2)$MHz; $\gamma_\perp = 2\pi(2.5 \pm 0.2)$MHz; $\kappa = 2\pi(0.9 \pm 0.1)$MHz. Based on these numbers the strong coupling condition of $\gamma_\perp, \kappa < g$ is met. A more detailed analysis is given in Supplementary Information V.

6.6. Strong coupling experiments involving ensembles of molecules

We now focus our attention on experiments involving ensembles of molecules, and again look at two experiments, one for information about the temporal oscillations, the other for an example of energy-level splitting.

For the first of these we look at an experiment by Vasa *et al.* [15], who investigated the interaction between dye molecules (TDBC aggregates dispersed in a 50 nm film of PVA) and the surface plasmon mode supported by a gold stripe array (i.e. a metallic grating). With an appropriate choice of array period they were able to probe the coupling between the excitonic resonance of the dye molecules at 2.1 eV and the surface plasmon mode of the gold surface. They probed the optical response of this system using a pump-probe set-up that had a femtosecond time resolution. In Figure 7a we reproduce some of their data for the differential reflectance of their sample as a function of time. They saw clear oscillations, indicating an exchange of energy between the molecules and the surface plasmon mode with a period of ~25 fs, in reasonable agreement with the extent of the energy splitting (110 meV).

For our second example, concerning energy splitting, we change from the excitonic resonance associated with the TDBC dye molecules investigated by Vasa *et al.* to a vibrational resonance, specifically that of the C=O bond. Vibrational resonances are usually measured in wavenumbers (cm^{-1}), and the C=O stretch has a resonance at $\sim 1730\,\text{cm}^{-1}$. One of the first reports involving strong coupling of this vibrational
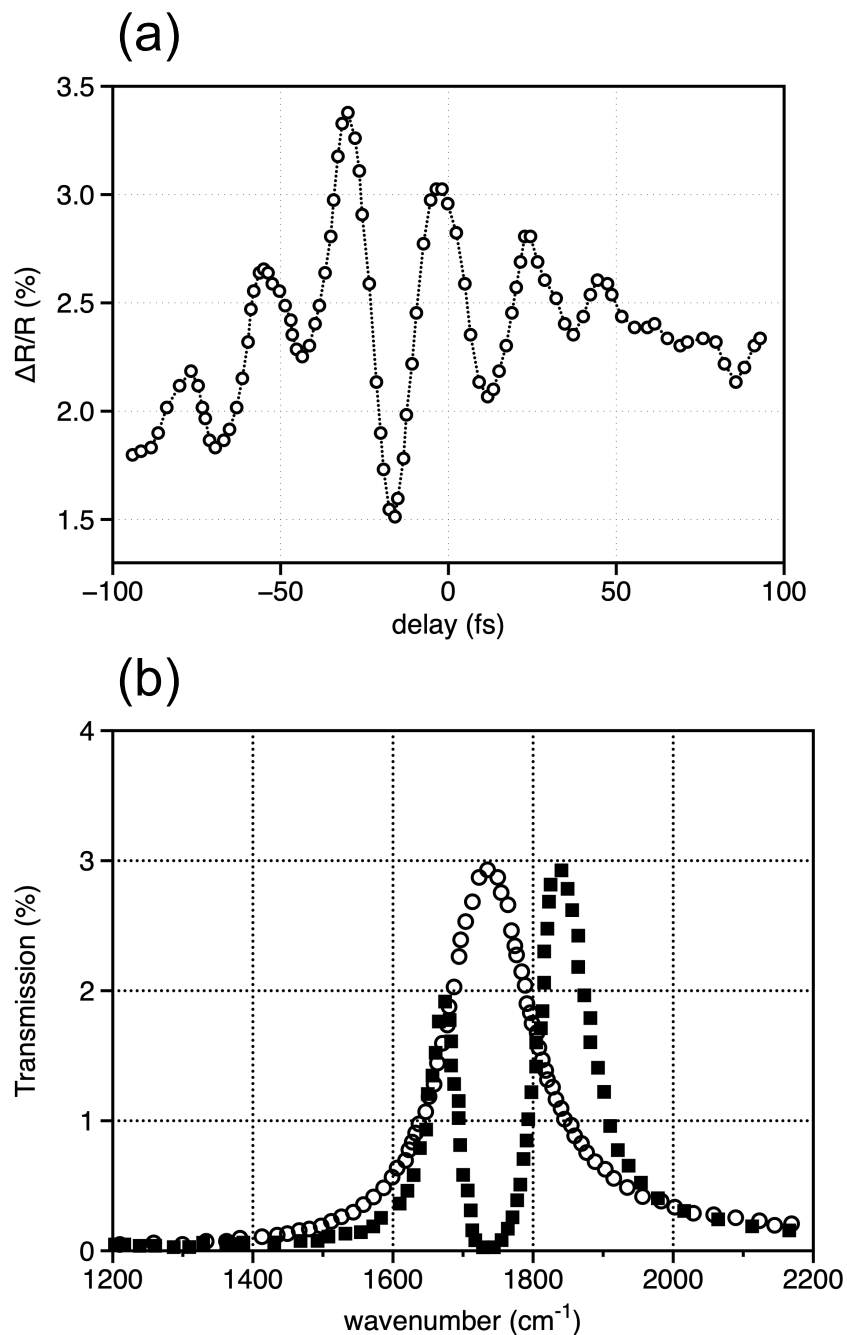
Figure 7. Ensembles of molecules: (a) Vasa *et al.* The differential reflectance is shown as a function of time. Clear oscillations are seen, with a period of approx. 25 fs. The oscillations for negative time delays arise due to dynamics induced by the probe beam. Data are adapted from [15]. The oscillation shows the exchange of energy between the molecules and the surface plasmon mode as a result of strong coupling. **(b) Shalabney *et al.*** The measured transmittance of a Fabry-Perot cavity comprising two 10 nm thick gold mirrors. The open circles show the (inferred) cavity transmittance in the absence of the molecular vibrational resonance, the filled squares show the transmittance when the cavity is filled with molecular resonators, in this case these are associated with the C=O bond. Data are adapted from [14]. The frequency splitting of the cavity transmission peak arising from strong coupling is clearly seen, although in this case a detailed analysis (including examination of angle-resolved measurements) is needed to show that the observed splitting is more than the result of 'simple' absorption.

resonance was that of Shalabney *et al.* [14] who made use of the large number of C=O bonds in a polymer (PVAc) film, using the polymer to provide the spacer layer in a planar Fabry-Perot cavity. With an appropriate choice of cavity thickness they ensured the lowest order cavity mode matched the frequency of the vibrational resonance. Further, by making the mirrors of the Fabry-Perot cavity thin enough (10 nm) they were able to measure the transmission, and thus probe the response of the system. Some of their transmission data are reproduced in Figure 7b. We see that the (inferred) transmittance of the cavity in the absence of a molecular vibrational resonance (circles), a single cavity transmission peak develops a split nature when the molecular resonance is present (squares). We can determine the extent of the splitting $(2g)$ to find $g = 85\,\mathrm{cm}^{-1}$. This compares with the molecular dephasing rate given by Shalabney *et al.* as 13 cm^{-1} and 65 cm^{-1} respectively; the strong coupling limit has thus been achieved. A more detailed analysis is given in Supplementary Information V.

7. Discussion

The goal of this paper has been to describe and explain strong coupling at an introductory level. We have tried to reduce the topic to the simplest systems, analogies and concepts. In what follows we discuss aspects that need to be considered if we are to better understand the complexities present in more complete and realistic investigations [33]. To begin, we can look at what still needs to be done from two perspectives, that of the electromagnetic mode(s) and of the molecular system(s).

First we focus on the electromagnetic modes. Throughout this article we have referred to the confined light mode as the cavity mode, and the detailed discussion of experiments in Section 6 has predominantly focused on strong coupling using cavities formed of two mirrors. As the topic of strong coupling has developed, new molecule-light systems have been introduced, each with their own benefits [34]. Environments for confined light can now be in the form of cavities, surfaces, nanoparticles, arrays, nanorods, gratings; often based on plasmonic platforms, but also employing dielectric systems. Dispersive material properties and complicated geometries lead to the possibility that molecules may interact with multiple confined light modes, each with its own Q factor, mode volume, and electric field profile [35].

When an explicit calculation for a system of one molecular resonator coupled to X photonic modes, which we write as $1 + X$, is undertaken, it is common practise to write down the resulting coupling matrix in $(1 + X) \times (1 + X)$ form, as demonstrated with the example of mechanical oscillators in Section 3[8]. It has been shown that this description may be lacking in cases where the photonic modes have large spatial extent or the molecules have a particularly large dipole moment (or equivalently, large oscillator strength); in these situations, it is necessary to include the interaction of the molecular mode with each photonic mode separately, resulting in a $2X \times 2X$ coupling matrix [36,37].

Accurately describing the electric field strength with high spatial resolution may be

---

[8]We used the $N + 1$ model in Section 3 to describe N molecules coupled to a single photonic mode, but the maths has precisely the same form for multiple photonic modes coupled to a single molecular mode. ω_{A} and ω_{B} must simply be associated with the appropriate modes

critical for complex nano-scale photonic environments such as those including very small metallic nanoparticles. Here non-local effects such as screening and Landau damping may also need to be considered [38].

Second, the molecular system. The simplification of treating the molecules as two-level systems is not always sufficient to describe molecular excitations, which may have multiple energy levels commensurate with the energies associated with the cavity field (particularly when considering vibrational degrees of freedom), and multiple mechanisms for loss and energy transfer within the molecular system. This is particularly important in the burgeoning field of polaritonic chemistry [39–41], in which it is hoped that the strong coupling of molecules to the vacuum field will change things such as reaction rates. The ideal scenario would be to treat a large number of molecules quantum-chemically, solvent included, at finite temperature, in a multi-modal, inhomogeneous photonic environment. This is computationally very demanding, but a good start has been made [42].

We should also consider what calculation methods might be best suited to model molecules strongly coupled to light. When complicated geometries and effects such as retardation must be taken into account, macroscopic QED offers a powerful method for describing the confined light modes [43]. A range of methods have been compared and contrasted elsewhere [33,41,44]. We might also note that although molecule-molecule interactions are often neglected, since these effects are generally small in comparison to molecule-light couplings [45], there may be systems in which they become important.

Finally we would like to mention some of the open challenges in the field of ensemble strong coupling. First there is the question of the extent to which single molecule properties are modified when a given molecule is collectively coupled to many others via strong coupling. An example of this is Raman scattering. Controversy in this area remains, despite a decade since the first report [46]. Recent results provide a somewhat mixed message [47,48], more work is clearly needed. Second, the role of dark states is – at the time of writing – seeing an intensive investigation. It appears as though dark states may be important in mediating interactions relevant to polaritonic chemistry [49,50]. Third, although the field was initially dominated by experimental reports, with little theoretical input, that situation is now changing, indeed, if anything theory now outstrips experiment! What would be useful is to bring experiment and theory closer together. As an example, studying how systems evolve as the number of molecules increases from 1 up to – say – 1000 in both experiment and theory, and in a controlled way, may offer a route to explore in a deep way the details of the strong coupling process. Such an approach will be demanding of both experimental and theoretical/numerical approaches, and may be daunting for systems where changes in chemistry are to be detected. Finally we note that there is scope to combine ensemble strong coupling with other recent developments in nanophotonics, for example by employing topological nanostructures [51]. Whatever the future for linking molecules with (virtual) light holds, it has already led to intensive experimental and theoretical activity and has both broadened our outlook and deepened our knowledge of light-matter interactions.

Acknowledgements

References

[1] Yuen-Zhou J, Menon VM. Polariton chemistry: Thinking inside the (photon) box. Proceedings of the National Academy of Sciences. 2019 Mar;116(12):5214–5216.

[2] Kimble HJ. Strong interactions of single atoms and photons in cavity QED. Physica Scripta. 1998;T76(1):127–137.

[3] Rabi II. Space quantization in a gyrating magnetic field. Physical Review. 1937;51(8):652.

[4] Deng H, Haug H, Yamamoto Y. Exciton-polariton bose-einstein condensation. Reviews of modern physics. 2010;82(2):1489.

[5] Orgiu E, George J, Hutchison J, et al. Conductivity in organic semiconductors hybridized with the vacuum field. Nature Materials. 2015;14(11):1123–1129.

[6] Vurgaftman I, Simpkins BS, Dunkelberger AD, et al. Negligible effect of vibrational polaritons on chemical reaction rates via the density of states pathway. The Journal of Physical Chemistry Letters. 2020;11(9):3557–3562.

[7] Imperatore MV, Asbury JB, Giebink NC. Reproducibility of cavity-enhanced chemical reaction rates in the vibrational strong coupling regime. The Journal of Chemical Physics. 2021;154(19):191103.

[8] Agarwal GS. Vacuum-field rabi splittings in microwave absorption by rydberg atoms in a cavity. Phys Rev Lett. 1984 Oct;53:1732–1734.

[9] Thomas PA, Tan WJ, Fernandez HA, et al. A new signature for strong light-matter coupling using spectroscopic ellipsometry. Nano Letters. 2020;20:6412–6419.

[10] Pippard AB. The physics of vibration. The Physics of Vibration. 2007;.

[11] Novotny L. Strong coupling, energy splitting, and level crossings: A classical perspective. American Journal of Physics. 2010;78(11):1199–1202.

[12] Törmä P, Barnes WL. Strong coupling between surface plasmon polaritons and emitters: a review. Reports on Progress in Physics. 2014;78(1):013901.

[13] Botzung T, Hagenmüller D, Schütz S, et al. Dark state semilocalization of quantum emitters in a cavity. Physical Review B. 2020;102(14):144202.

[14] Shalabney A, George J, Hutchison J, et al. Coherent coupling of molecular resonators with a microcavity mode. Nature Communications. 2015 Jan;6(1):1–6.

[15] Vasa P, Wang W, Pomraenke R, et al. Real-time observation of ultrafast rabi oscillations between excitons and plasmons in metal nanostructures with j-aggregates. Nature Photonics. 2013 Jan;7(2):128–132.

[16] Tsargorodska A, Cartron ML, Vasilev C, et al. Strong coupling of localized surface plasmons to excitons in light-harvesting complexes. Nano Letters. 2016 Oct;16(11):6850–6856.

[17] Rider MS, Arul R, Baumberg JJ, et al. Theory of strong coupling between molecules and surface plasmons on a grating. arXiv preprint arXiv:220512745. 2022;.

[18] Savona V, Andreani L, Schwendimann P, et al. Quantum well excitons in semiconductor microcavities: Unified treatment of weak and strong coupling regimes. Solid State Communications. 1995;93(9):733–739.

[19] Laussy FP, Del Valle E, Tejedor C. Strong coupling of quantum dots in microcavities. Physical review letters. 2008;101(8):083601.

[20] Auffèves A, Gerace D, Gérard JM, et al. Controlling the dynamics of a coupled atom-cavity system by pure dephasing. Physical Review B. 2010;81(24):245419.

[21] Forn-Díaz P, Lamata L, Rico E, et al. Ultrastrong coupling regimes of light-matter interaction. Reviews of Modern Physics. 2019;91(2):025005.

[22] Frisk Kockum A, Miranowicz A, De Liberato S, et al. Ultrastrong coupling between light and matter. Nature Reviews Physics. 2019;1(1):19–40.

[23] Ciuti C, Bastard G, Carusotto I. Quantum vacuum properties of the intersubband cavity polariton field. Physical Review B. 2005;72(11):115303.

[24] Mueller NS, Okamura Y, Vieira BGM, et al. Deep strong light-matter coupling in plasmonic nanoparticle crystals. Nature. 2020;583:780.

[25] Zewail AH. Laser selective chemistry—is it possible? Physics Today. 1980;33(11):27–33.

[26] Griffiths DJ. Introduction to Electrodynamics. 3rd ed. Upper Saddle River: Prentice-Hall; 1999.

[27] Dintinger J, Klein S, Bustos F, et al. Strong coupling between surface plasmon-polaritons and organic molecules in subwavelength hole arrays. Physical Review B. 2005 Jan; 71(3):035424.

[28] Eizner E, Martínez-Martínez LA, Yuen-Zhou J, et al. Inverting singlet and triplet excited states using strong light-matter coupling. Science Advances. 2019;5(12):eaax4482.

[29] Chikkaraddy R, de Nijs B, Benz F, et al. Single-molecule strong coupling at room temperature in plasmonic nanocavities. Nature. 2016 Jun;535(7610):127–130.

[30] Thompson RJ, Rempe G, Kimble HJ. Observation of normal-mode splitting for an atom in an optical cavity. Phys Rev Lett. 1992 Feb;68:1132–1135.

[31] Kaluzny Y, Goy P, Gross M, et al. Observation of self-induced rabi oscillations in two-level atoms excited inside a resonant cavity: The ringing regime of superradiance. Phys Rev Lett. 1983 Sep;51:1175–1178.

[32] Orfanakis K, Rajendran SK, Walther V, et al. Rydberg exciton–polaritons in a cu2o microcavity. Nature Materials. 2022;21(7):767–772.

[33] Sánchez-Barquilla M, Fernández-Domínguez AI, Feist J, et al. A theoretical perspective on molecular polaritonics. arXiv preprint arXiv:220102827. 2022;.

[34] Baranov DG, Wersall M, Cuadra J, et al. Novel nanostructures and materials for strong light–matter interactions. Acs Photonics. 2018;5(1):24–42.

[35] Menghrajani KS, Barnes WL. Strong coupling beyond the light-line. ACS Photonics. 2020;7(9):2448–2459.

[36] Richter S, Michalsky T, Fricke L, et al. Maxwell consideration of polaritonic quasi-particle hamiltonians in multi-level systems. Applied Physics Letters. 2015;107(23):231104.

[37] Balasubrahmaniyam M, Genet C, Schwartz T. Coupling and decoupling of polaritonic states in multimode cavities. Physical Review B. 2021;103(24):L241407.

[38] García de Abajo FJ. Nonlocal effects in the plasmons of strongly interacting nanoparticles, dimers, and waveguides. The Journal of Physical Chemistry C. 2008;112(46):17983–17987.

[39] Ribeiro RF, Martínez-Martínez LA, Du M, et al. Polariton chemistry: controlling molecular dynamics with optical cavities. Chemical science. 2018;9(30):6325–6339.

[40] Feist J, Galego J, Garcia-Vidal FJ. Polaritonic chemistry with organic molecules. ACS Photonics. 2018;5(1):205–216.

[41] Fregoni J, Garcia-Vidal FJ, Feist J. Theoretical challenges in polaritonic chemistry. ACS Photonics. 2021;.

[42] Groenhof G, Climent C, Feist J, et al. Tracking polariton relaxation with multiscale molecular dynamics simulations. The Journal of Physical Chemistry Letters. 2019 Aug; 10(18):5476–5483.

[43] Feist J, Fernández-Domínguez AI, García-Vidal FJ. Macroscopic qed for quantum

nanophotonics: emitter-centered modes as a minimal basis for multiemitter problems. Nanophotonics. 2021;10(1):477–489.

[44] Herrera F, Owrutsky J. Molecular polaritons for controlling chemistry with quantum optics. The Journal of chemical physics. 2020;152(10):100902.

[45] Nečada M, Martikainen JP, Törmä P. Quantum emitter dipole–dipole interactions in nanoplasmonic systems. International Journal of Modern Physics B. 2017;31(24):1740006.

[46] Shalabney A, George J, Hiura H, et al. Enhanced raman scattering from vibro-polariton hybrid states. Angewandte Chemie International Edition. 2015 Jun;54(27):7971–7975.

[47] Ahn W, Simpkins BS. Raman scattering under strong vibration-cavity coupling. The Journal of Physical Chemistry C. 2021;125(1):830–835.

[48] Menghrajani KS, Chen M, Dholakia K, et al. Probing vibrational strong coupling of molecules with wavelength-modulated raman spectroscopy. Advanced Optical Materials. 2021 Nov;10(3):2102065.

[49] del Pino J, Feist J, Garcia-Vidal FJ. Signatures of vibrational strong coupling in raman scattering. The Journal of Physical Chemistry C. 2015 Dec;119(52):29132–29137.

[50] Botzung T, Hagenmüller D, Schütz S, et al. Dark state semilocalization of quantum emitters in a cavity. Phys Rev B. 2020 Oct;102:144202.

[51] Rider MS, Palmer SJ, Pocock SR, et al. A perspective on topological nanophotonics: Current status and future challenges. Journal of Applied Physics. 2019;125(12):120901.

[52] Barnes WL, Horsley SAR, Vos WL. Classical antennas, quantum emitters, and densities of optical states. Journal of Optics. 2020;22:073501.

[53] Rodriguez SRK. Classical and quantum distinctions between weak and strong coupling. European Journal of Physics. 2016;37(2):025802.

[54] Lagendijk A. Vibrational relaxation studied with light. Boston, MA: Springer US; 1993.

[55] Grynberg G, Aspect A, Fabre C. Introduction to quantum optics. Cambridge University Press; 2010.

[56] Steck DA. Cesium d line data. University of Oregon; 1998.

[57] Ujihara K. Spontaneous emission and the concept of effective area in a very short optical cavity with plane-parallel dielectric mirrors. Japanese Journal of Applied Physics. 1991; 30:L901–L903.

[58] Long JP, Simpkins BS. Coherent coupling between a molecular vibration and fabry-perot optical cavity to give hybridised states in the strong coupling limit. ACS Photonics. 2015; 2:130–136.

[59] Medina I, García-Vidal FJ, Fernández-Domínguez AI, et al. Few-mode field quantization of arbitrary electromagnetic spectral densities. Phys Rev Lett. 2021 Mar;126:093601.

[60] Feist J, Fernández-Domínguez AI, García-Vidal FJ. Macroscopic qed for quantum nanophotonics: emitter-centered modes as a minimal basis for multiemitter problems. Nanophotonics. 2021;10(1):477–489.

[61] Cuartero-González A, Manjavacas A, Fernández-Domínguez AI. Distortion of the local density of states in a plasmonic cavity by a quantum emitter. New Journal of Physics. 2021 jul;23(7):073011.

[62] Wang S, Chervy T, George J, et al. Quantum yield of polariton emission from hybrid light-matter states. Journal of Physical Chemistry Letters. 2014;5:1433–1439.

[63] Fox M. Quantum optics: an introduction. 1st ed. Oxford University Press; 2006.

[64] Bonifacio R, Lugiato LA. Optical bistability and cooperative effects in resonance fluorescence. Phys Rev A. 1978 Sep;18:1129–1144.

[65] Pinkse P, Rempe G. 8. single atoms moving in a high-finesse cavity. In: van Zee RD, Looney JP, editors. Cavity-enhanced spectroscopies. (Experimental Methods in the Physical Sciences; Vol. 40). Academic Press; 2003. p. 255–295.

[66] Tanji-Suzuki H, Leroux ID, Schleier-Smith MH, et al. Chapter 4 - interaction between atomic ensembles and optical resonators: Classical description. In: Arimondo E, Berman P, Lin C, editors. Advances in atomic, molecular, and optical physics. (Advances In Atomic, Molecular, and Optical Physics; Vol. 60). Academic Press; 2011. p. 201–237.

Something from nothing: linking molecules with virtual light
Supplementary Information

SI I. Weak coupling

If the strong coupling criterion (Equation (3)) is not met, i.e. if the rate of energy exchange is not the fastest rate, then the effect of the cavity is to act as a bath into which the excitation energy of the molecule is lost irreversibly. In this situation we are in what is known as the weak coupling regime, and the rate at which this spontaneous emission (SpE) takes place, Γ, is given by Fermi's golden rule [52].

$$\Gamma = \frac{2\pi}{\hbar^2} |\vec{\mu}.\vec{E}|^2 = 2\pi g^2. \tag{I1}$$

This is the spontaneous emission rate, as modified by the presence of the cavity [52]. In free space $\Gamma_0 = 2\gamma$, see Supplementary Information IV. The value of E here is that of the vacuum, **as 'dressed' by the cavity**. For there to be a significant change in the SpE rate from the free space value, and yet for us not be in the strong coupling regime, we need,

$$\kappa >> g \gtrsim \gamma. \tag{I2}$$

SI II. Two coupled mechanical oscillators

For completion we give the derivation for the coupling matrix of two coupled mechanical oscillators, as it commonly presented in literature. We recover the expected result for $N = 1$ when compared to the $N + 1$ system in Section 3.

$$m\ddot{x}_A(t) = -k_A x_A(t) - K_c \left(x_A(t) - x_B(t) \right)$$
$$m\ddot{x}_B(t) = -k_B x_B(t) + K_c \left(x_A(t) - x_B(t) \right). \tag{II1}$$

For solutions of the form $x_i(t) = x_i^0 e^{-i\omega t}$ (i.e. assuming the total system oscillates with a single frequency), the coupled linear equations for x_A^0 and x_B^0 can be written in matrix form,

$$\mathbf{M} \begin{pmatrix} x_A^0 \\ x_B^0 \end{pmatrix} = 0, \quad \text{where} \quad \mathbf{M} = \begin{pmatrix} -\frac{k_A + K_c}{m} + \omega^2 & \frac{K}{m} \\ \frac{K_c}{m} & -\frac{k_B + K}{m} + \omega^2 \end{pmatrix}. \tag{II2}$$

Non-trivial solutions exist for $\det(\mathbf{M}) = 0$, which leads to the condition that

$$\omega_{\pm}^2 = \frac{1}{2} \left[\omega_A^2 + \omega_B^2 \pm \sqrt{\left(\omega_A^2 - \omega_B^2 \right)^2 + 4\Gamma^2} \right], \tag{II3}$$

where

$$\omega_A = \sqrt{\frac{k_A + K_c}{m}}, \quad \omega_B = \sqrt{\frac{k_B + K_c}{m}}, \quad \Gamma = \frac{K_c}{m}. \tag{II4}$$

We note that ω_A and ω_B are the frequencies of each oscillator if the position of the other oscillator were to remain fixed. For $k_i \gg K_c$, $\omega_i \approx \omega_i^0$, the natural frequencies of the uncoupled oscillators. Properties such as the magnitude of the Rabi splitting and conditions for strong coupling are not affected by this assumption, and the relative magnitudes of these values are typically what is found in molecule-light interactions, and so we use this condition for the rest of this section. We see in Figure 3b that the introduction of the third spring results in an avoided crossing at resonance. The band gap at resonance is given by $\omega_+^2 - \omega_-^2 = 2K_c/m$. The allowed modes can be set by changing the spring constants of the system. At resonance, such that $\omega_A = \omega_B$, in the uncoupled system we would see the two masses oscillating with the same frequency but arbitrary relative phase. In the coupled system, the two normal modes are given by: the masses oscillating perfectly in phase (lower energy) or out of phase (higher energy).

SI III. Classical vs quantum coupling matrix

The classical coupling matrix for two coupled oscillators, i.e. $N = 1$ from Equation (7), written in terms of frequencies is,

$$\mathbf{M} = \begin{pmatrix} -\omega_A^2 + \omega^2 & \Gamma \\ \Gamma & -\omega_B^2 + \omega^2 \end{pmatrix}. \tag{III1}$$

Dividing the first row of the classical coupling matrix by $\omega_A + \omega$ and the second row by $\omega_B + \omega$ [9],

$$\mathbf{M} = \begin{pmatrix} \frac{\omega^2 - \omega_A^2}{\omega_A + \omega} & \frac{\Gamma}{\omega_A + \omega} \\ \frac{\Gamma}{\omega_B + \omega} & \frac{\omega^2 - \omega_B^2}{\omega_B + \omega} \end{pmatrix}. \tag{III2}$$

Factorising, multiplying by -1, and defining $g = -\Gamma/\tilde{\omega}$ where $\tilde{\omega} = \omega + \omega_{A,B}$, we recover the quantum coupling matrix of Equation (13),

$$\mathbf{M} = \begin{pmatrix} \omega_A - \omega & g \\ g & \omega_B - \omega \end{pmatrix}. \tag{III3}$$

This comparison of classical and quantum coupling matrices may be extended to systems with losses [53]. As with the classical model, when N oscillators of frequency ω_A are included, an effective coupling constant $g_N = \sqrt{N}g$ can be introduced or the full $N + 1$ system can be diagonalised so as to include the dark states.

---

[9]This 'trick' can be undertaken by remembering that this matrix represents a set of simultaneous equations represented as $\mathbf{Mx} = 0$, as per Equation (6), and so the rows of the matrix can be divided by different expressions and still describe the correct equations of motion.

SI IV. Rate definitions

The three rates, the atom-cavity coupling rate g, the atomic decay rate γ and the cavity decay rate κ are essential in our understanding of molecular strong coupling. Here we wish to focus on how these rates are defined since different specialist areas, and indeed different authors within a specialism, sometimes define things differently, a not uncommon but nonetheless confusing situation.

IV.1. Atomic/Molecular decay rates

Care is needed here when considering which atomic decay rate is appropriate. Strong coupling involves a coherent exchange of energy between the material (atom) and the optical field (cavity mode), it is thus the decay rate of the atomic coherence that is relevant here. As so often in physics, this can lead to an unexpected factor of two appearing. For a simple atomic two-level system whose linewidth is determined by the radiative lifetime[10] then the decay rate of the atomic coherence (i.e. the transition dipole moment, an amplitude) is half the spontaneous emission decay rate (an intensity) [54]. In the atomic optics community these rates are referred to respectively as the transverse and longitudinal rates, $\gamma_\perp$, $\gamma_\parallel$, with $\gamma_\perp = \gamma_\parallel/2$, with the nomenclature referring to the evolution of a two level system as described using the Bloch-sphere, originally developed in the context of nuclear magnetic resonance (NMR). For those readers more familiar with nanophotonics the quantity they will be familiar with is the spontaneous emission rate Γ_0, something that allows the number of photons emitted per second to be calculated, i.e. an intensity, thus $\gamma = \Gamma_0/2$. Note that the FWHM linewidth for the case of a transition that is well described by the Lorentz oscillator (LO) model is 2γ where $i\gamma\omega$ is the damping term in the LO model.

IV.2. Cavity decay rate

A similar confusion is possible regarding the cavity decay rate. As with the atomic decay rate, in this case it is decay of the field coherence κ that matters, so the relevant decay rate is half the cavity linewidth [55], i.e. $2\kappa = K$, where $K = \omega_c/Q$, ω_c being the resonance frequency of the cavity and Q the quality factor of the cavity resonance. Confusingly the value of ω_c/Q is often assigned to the variable κ.

SI V. Numerical analysis of experiments

V.1. Numerical analysis - Atom Optics

Here we look at the numbers for the atom optics experiment of Kaluzny *et al.* [31].

First let us check κ. The authors give the cavity finesse as $F = 8 \times 10^4$ which, using $Q = \pi c/\lambda_0\kappa = 2FL/\lambda_0$, where λ_0 is the wavelength associated with the transition ($\lambda_0 =$ 852 nm) and L is the cavity length (1.0 mm), gives $\kappa = 2\pi(0.9 \pm 0.1)$MHz as required, and we can also find $Q = 1.9 \times 10^8$. This compares to the Q of the transition of $352\,\mathrm{THz}/2.5\,\mathrm{MHz} = 1.4 \times 10^8$, achieving such high Q-factors for the cavity modes was a major challenge in atom optics. The cavity volume for this type

---

[10]We also note that there are implications here regarding the effect of inhomogeneous broadening of strongly coupled transitions.

of confocal mode is given by $V = \pi w_0^2 L/4$, where w_0 is the beam waist, given by Thompson *et al.* as 50 μm. The volume is thus $V = 1.96 \times 10^{-12}\,\mathrm{m}^3$. Using (20) we can calculate the associated vacuum field strength as 80 V$\cdot$m^{-1}. For the dipole moment we can consult Steck [56] who gives the (effective) dipole moment as $1.7 \times 10^{-29}\,\mathrm{C}\cdot\mathrm{m}$ ($\equiv 5.2$ D (Debye)). Using (22) we thus find $g = 2\pi(2.1)\,\mathrm{MHz}$ which, given that we have ignored the variation of the field across the cavity mode etc. is in pretty good agreement with the measured value of $g = 2\pi(3.2)\,\mathrm{MHz}$.

V.2. Numerical analysis - Vibrational Strong Coupling

Here we look at the numbers for the molecular ensemble system of Shalabney *et al.* [14]. In the infrared it is common to use wavenumbers (cm^{-1}) for frequencies. In wavenumbers the C=O vibrational resonance of interest occurs at 1730cm^{-1}.

In the infrared it is usual to work with wavenumbers, so that the C=O transition occurs at 1734 cm^{-1}. Shalabney *et al.* give the value of the splitting $\Omega_R = 2g_N$ as 167 cm^{-1} (equivalent to 20.7 meV). This gives $2g_N = 84$ cm^{-1}. The cavity and molecule damping rates can be estimated as follows. For the cavity the FWHM linewidth of the empty cavity is found from the prediction by Shalbney *et al.* to be 130 cm^{-1} giving a value for the cavity dephasing rate of $\kappa = \mathrm{FMHM}/2 = 65$ cm^{-1}. The factor of 2 is because κ is a dephasing rate [55], (see also Supplementary Information IV). The cavity quality factor is thus ~ 13. For the molecular dephasing rate, an IR spectrum for the transmission of the C=O transition is also given by Shalabney *et al.*. Using a simple Lorentz oscillator model for the associated permittivity we can extract the value of γ, we find $\gamma = 16$ cm^{-1}, in reasonable agreement with the 13 cm^{-1} found by Shalabney *et al.*. Based on these numbers the strong coupling condition of $\gamma, \kappa < g$ is met. The cavity volume for this type of cavity can be estimated from the reflectivity of the mirrors [57]. We estimated the reflectivity using a Fresnel approach, making use of reasonable estimates for the material parameters. We find an average reflectivity of 0.8, allowing us to estimate the cavity volume as 300 μm^3. The vacuum field strength is thus 1.7×10^3 V m^{-1}. (This value is higher than that given by Shalabney *et al.* (6.3×10^3 V m^{-1}) since those authors assumed the volume to be equal to that of a diffraction limited cube. The number density of C=O bonds can be estimated from the density of PVAc (1.18 g/cm^3) and the molecular weight of the PVAc repeat unit (86 g mol^{-1}) giving a number density of 8×10^{27} bonds m^{-3}. In the cavity volume there are thus $\sim 2 \times 10^{12}$ C=O bonds. Finally, the dipole moment can be estimated from the oscillator strength obtained from the same Lorentzian oscillator fit to the transmittance data we used above to extract the dephasing rate. We find the dipole moment to be 0.3 D.

Let us use the numbers above to estimate the vale of g and g_N. Making use of Equations (21) and (22) we find; $g \approx 10^{-4}$cm^{-1} and $g_N = 110$cm^{-1}. We note two interesting points. First, the value of the single bond coupling strength of 1×10^{-4}cm^{-1} is very small, orders of magnitude less than the dephasing rates. Second, strong coupling ***is*** possible through the collective action of the $\sim 2 \times 10^{12}$ C=O bonds involved, giving $g_N = 140$cm^{-1}, which is nearly twice the measured value of 84 cm^{-1}. Given the large number of estimates we have made this is a good agreement. A much more refined analysis of a similar and contemporaneous experiment is given by Long *et al.* [58].

SI VI. Densities of states, spectral densities, cooperativity, and the Purcell factor

We have focused our attention on the electric field as a way to characterise the 'light' element in strong light-matter coupling. Whilst this seems to us at least to us to provide the strongest intuitive perspective, many other frameworks for light-matter coupling are in use and they are discussed and contrasted here.

VI.1. Densities of states ($\rho_{\mathrm{P}}(\omega)$)

The modification of spontaneous emission that occurs when a molecule is placed inside a cavity is often the domain of nanophotonics, and the modification is usually discussed in terms of the local density of optical states. In essence, for an excited molecule to emit a photon there must be at least one mode in the environment of the molecule into which emission can take place. If the mode is tightly confined g will be significant and the emission rate will be enhanced (see eqn. (I1)), a useful tactic in producing single photon sources. If there is no mode then the emission will be inhibited, as for example inside a photonic band gap. It is the projected (also known as partial) local density of states that is important [52] since this takes account of the relative orientation of the dipole moment and the electric field vector (hence projected), and the position of the dipole within the field (hence local). It is natural to ask whether the strong coupling condition can be expressed in terms of the projected local density of optical states (PLDOS).

To make progress here we need to recognise that we have been rather lax about the coupling constant g. To calculate the interaction strength rigorously we should take account of the way the vacuum field strength varies with frequency, i.e. $g = g(\omega)d\omega = (\mu/\hbar)E(\omega)d\omega$. In our expression for the vacuum field strength we already noted that the mode volume is the volume occupied by our (assumed) single mode. Now, the (projected) density of optical states, ρ_{P}, is the number of states per unit volume, per unit frequency. Recognising this we can then identify $\rho_{\mathrm{P}}d\omega$ as being $1/V$ because we know we have just one mode occupying the mode volume (this was the assumption we made in deriving eqn. (21). With just one mode present it doesn't really make sense to write our coupling rate in terms of a density of states, nonetheless we can do so by making use of eqn. (21) to write,

$$g = \mu\sqrt{\frac{\omega\rho_{\mathrm{P}}(\omega)d\omega}{2\varepsilon_0\hbar}}. \tag{VI1}$$

Recalling now that for strong coupling we need $\kappa, \gamma < g$ we can now see that there is no special condition on the density of states for strong coupling; yes, the PLDOS 'determines' the coupling strength, but whether that coupling strength is sufficient for strong coupling is dictated by requiring $\kappa, \gamma < g$.

VI.2. Spectral density $J(\omega)$

Another framework, similar in many ways to the density of states, is the spectral density $J(\omega)$[59–61]. In contrast to the mode density, the spectral density includes the dipole moment, i.e. in some sense it incorporates the coupling strength. The spectral

density, just like the local density of states, is often a convenient framework with which to describe light-matter interactions. In terms of the notation used here,

$$J(\omega)d\omega = g(\omega)^2 d\omega = \frac{\mu^2\omega}{2\varepsilon_0\hbar}\,\rho_{\mathrm{P}}(\omega)d\omega. \tag{VI2}$$

For completeness we note that in the weak coupling regime Fermi's golden rule can be written in terms of the spectral density as $\Gamma = 2\pi J(\omega)$.

Interlude Our models have all been very simplistic. For example, frequently more than one electromagnetic mode may be present [35,36], and as another example we have ignored the spatial variation of the field within the mode volume [62]. In such cases $\rho_{\mathrm{P}}(\omega)$ and $J(\omega)$ may have their advantages. At root however in the physics of strong coupling phenomena is the role of the electric (vacuum) field and it is to keep this physical origin prominent that we have chosen to stick with it here. Depending on the complexity of the situation, $\rho_{\mathrm{P}}(\omega)$ and $J(\omega)$ may be calculated using either a Green function approach or numerically. Perhaps the most complete description involves what is known as 'macroscopic QED' [43]. However, our simple picture is informative and allows us to quickly build physical intuition of strong coupling physics.

Two other concepts are encountered in light-matter interactions, albeit in very different contexts, the Purcell factor, and the cooperativity; they are associated with very different realms, but turn out to be the same thing. For completeness, and to show how they relate to the parameters already discussed.

VI.3. Purcell factor ($\mathrm{F_P}$)

The Purcell factor is a measure of the extent to which the electromagnetic environment around an emitter alters the emitter's spontaneous emission (SpE) rate. It is a convenient measure of the effect of environment on the emission from a source embedded in a nano-structure, it is in common use in the nanophotonics community. The Purcell factor is defined as the ratio of the SpE rate in the presence of the cavity, Γ_{cav}, to the SpE rate in the same host material but in the absence of the cavity, Γ_0. Assuming for the moment that the host medium is vacuum, then we have [63],

$$\mathrm{F_P} = \frac{\Gamma_{\mathrm{cav}}}{\Gamma_0} = \frac{6\pi Q c^3}{\omega^3 V}, \tag{VI3}$$

where the expression on the r.h.s. is a standard result, and Q and V are the quality factor of the cavity mode and the mode volume, as before. We can use eqn. (VI1) to write the Purcell factor in terms of g rather than V. We can then make use of the standard expression for the free-space decay rate [63],

$$\Gamma_0 = 2\gamma = \frac{\mu^2\omega^3}{3\pi\varepsilon_0\hbar c^3}, \tag{VI4}$$

where the fact that we have used 2γ, rather than γ is discussed in Supplementary Information section IV. Lastly we need to note that $Q = \omega/2\kappa$ (again, the factor of 2

is discussed in Supplementary Information section IV). Combining these we find that,

$$F_P = \frac{g^2}{\kappa\gamma} = C.$$

(VI5)

The C in this equation is known as the cooperativity.

VI.4. Cooperativity (C)

The concept of cooperativity was it seems was first established in the area of optical bistability [64], but has since been adopted by the atom optics community [65,66]. Recalling the discussion above about the atom and cavity decay rates, we note that in terms of the more familiar experimental quantities, Γ_0 and K the single and N-atom cooperativities are,

$$C = \frac{4g^2}{\Gamma_0 K},$$

(VI6)

$$C = \frac{4Ng^2}{\Gamma_0 K}.$$

(VI7)

Definitions of the cooperativity in the literature vary, as do the way the cooperativity relates to the Purcell factor. These variations typically involve factors of two and originate from the way different authors chose to define and use the decay rates; the reader is warned! As an example, the oft-quoted Kimble gives $C = g^2/2\gamma\kappa$, for which $F_P = 2C$ [2]. The choice we make here is the same as that of Tanji-Suzuki *et al.* [66], This choice is convenient when considering data from experiments where it is often the spectral widths that are important.